# Polymer Films on Electrodes

## XXVII. Electrochemical and Ellipsometric Measurements of a Viologen-Siloxane Polymer Film: Deposition, Solvent Swelling, Oxidation-State-Dependent Thickness, and Charge Transport

**Larry J. Kepley* and Allen J. Bard****

*Department of Chemistry and Biochemistry, The University of Texas at Austin, Austin, Texas 78712, USA*

ABSTRACT

*In situ* ellipsometry was used to study the electrodeposition of the viologen-based redox polymer formed by electroreduction of *N,N'*-bis[-3-(trimethoxysilyl)propyl]-4,4'-bipyridinium dichloride (**I**) at Pt electrodes. The importance of dimerization of the 1+ species in the film was demonstrated by comparing voltammetric results for thin films of the polymer with equations derived for the current, peak potential, and limiting shape of thin layer, linear sweep voltammograms for a kinetically reversible couple, where one form of the couple undergoes fast reversible dimerization. The complex refractive index and viologen concentration for solvent swollen films were determined for the 2+ and 1+ states of the viologen groups during film growth. The polymer deposited isotropically to thicknesses of ≤400 nm (2+ state). High quality films for ellipsometric measurements were also formed by spin-coating the electrode with ethanolic solutions of **I**. The film optical constants, degree of film swelling by solvent sorption, and changes in swelling associated with reduction in blank electrolyte solution were determined from least squares analysis of data for multiple angles of incidence, without resorting to auxiliary measurements. Reduction caused film shrinkage of about 25%. Modeling of transient ellipsometric data for large potential steps was used to test the theory that electron transport represents a diffusion process. Theoretical curves were calculated by treating the film as a system of stratified layers whose optical constants were given by effective medium theory using the refractive indexes of completely reduced and oxidized films and simulated thin layer conversion profiles (*i.e.*, gradients) for diffusional transport. During film reduction, hopping of electrons (between 1+ and 2+ centers) effectively followed a diffusion model, with reduction proceeding outward from the electrode/film interface. Film oxidation back to the 2+ state was slower and required film reswelling, which lagged the extent of oxidation during both fast and slow conversions (*i.e.*, during potential steps and sweeps). Ellipsometric data provided the first direct evidence that film expansion driven by a redox process can impede charge transport.

Research of polymer modified electrodes (PMEs) is now a fairly mature area.[1,2] Electron transport in polymers containing bound redox sites (redox polymers) occurs by electron hopping between neighboring redox centers.[3] In the simplest case, where the negligible resistive potential drop or phase changes occur in the film, electron transport can be represented as a diffusion process with an effective diffusion coefficient ($D_e$).[4] However, electron transport during electrochemical conversion of redox polymers can be influenced by coupled processes, such as counterion migration or changes in levels of film swelling by electrolyte solution, to yield an overall observed charge-transport rate ($D_{ct}$). Film swelling by solution is important,[5-9] because electron transfer and ion transport both require local chain motion and conformational freedom. Segmental chain motion controls the collision frequency of redox centers[10,11] and also creates free volume necessary for ion mobility.[12] The degree of swelling can vary from about 15 to 180% for nonpolar aprotic polymers[13-16] to as much as 100-fold for a protonated polar polymer.[17]

In studies of PMEs the question typically arises: does $D_{ct} = D_e$, or does $D_{ct}$ represent limitations from coupled processes? The presence of counterion or film swelling limitations in redox polymers is not easily discernible from voltammetric measurements alone. PMEs suspected of being counterion-transport limited can also give linear chronoamperometric and chronocoulometric plots indicative of diffusion-limited transport.[18,19] Electrolyte dependencies can suggest the presence of ion transport limitations, but the nature of the electrolyte solution can also affect intrinsic electron hopping rates by its influence on chain packing and dynamics.[20] Furthermore, $D_{ct}$ can be larger than $D_e$ due to field-enhanced electron hopping (*i.e.*, electron migration),[21] if a significant electric field develops across the film as a result of poor ion mobility,[22] which again raises the possibility of nondiffusional electron transport.

We discuss here simultaneous voltammetric and ellipsometric measurements of film swelling and conversion of the siloxane-paraquat redox polymer ($PQ^{2+/+}$) formed by hydrolysis and condensation of *N,N'*-bis[-3-(trimethoxysilyl)propyl]-4,4'-bipyridinium dichloride, **I**.[23,24] We

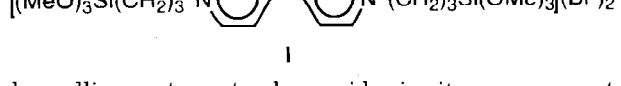


**I**

show ellipsometry not only provides *in situ* measurements of film thickness ($d$) as a function of oxidation state, which can give information about the effects of changes in film swelling on $D_{ct}$, but that its sensitivity to redox conversion gradients can be used to verify optically that diffusional transport prevailed. Ellipsometry has been used previously to determine whether conversion proceeded either outward from the electrode/film interface or inward from the film/solution interface during electrochemical interconversion of metal oxides,[25] conducting polymers,[26-28] and polythionine.[29] The work presented here is the first ellipsometric study of a highly swollen redox polymer.

$PQ^{2+/+}$ was chosen as a good model system for the following reasons: (*i*) its chemical stability and intense coloration upon reduction allowed the precision and sensitivity necessary to determine the conversion gradient. (*ii*) Film conversion rates for this polymer yield some of the largest $D_{ct}$ values yet reported, making the level of film swelling and the *in situ* redox site concentration for this system especially interesting. $D_{ct}$ cannot be determined without knowledge of the solvent-swollen film thickness. (*iii*) $PQ^{2+/+}$ films display almost ideal thin-layer behavior and the viologen centers form dimers when reduced (Eq. 1 and 2), so $PQ^{2+/+}$

$$PQ^{2+} + e^- \rightleftharpoons PQ^+ \qquad [1]$$

$$2PQ^+ \underset{k_b}{\overset{k_f}{\rightleftharpoons}} (PQ^+)_2 \qquad [2]$$

films were suitable for testing the theory for thin-layer voltammetry of reversible electron transfer with following dimerization. Reversible dimerization has been seen for other polymer-bound organic redox groups, including 10-methylphenothiazine (PTZ),[30] tetrathiafulvalene (TTF),[3b] and tetracyanoquinodimethane (TCNQ).[31] Theory has been presented for the case of a following irreversible dimeriza-

* Electrochemical Society Student Member.
** Electrochemical Society Fellow.

**Table I. $PQ^{2+}$ film thicknesses and optical constants for various ambient phases.**

| Film | Ambient phase | $n_1$ | $k$ | $d$(nm) | $C^*_{PQ^{2+}}$ ($M$) |
|---|---|---|---|---|---|
| A[a] | $N_2$ gas | 1.56 ± 0.12 | 0.04 ± 0.04 | 80 ± 10 | 1.9 ± 0.2 |
| | $H_2O$ vapor (*ca.* 100% humidity) | 1.41 ± 0.005 | 0.005 ± 0.005 | 189 ± 5 | 0.80 ± 0.03 |
| | MeCN-vapor | 1.55 ± 0.01 | 0.005 ± 0.005 | 125 ± 5 | 1.22 ± 0.06 |
| | 1.0 $M$ KCl soln-vapor | 1.47 ± 0.01 | 0.005 ± 0.005 | 149 ± 5 | 1.02 ± 0.05 |
| | 1.0 $M$ KCl soln | 1.46 ± 0.01 | 0.005 ± 0.005 | 145 ± 5 | 1.05 ± 0.05 |
| B[b] | $N_2$ gas | 1.77 ± 0.02 | 0.005 ± 0.005 | 88 ± 3 | — |
| | $H_2O$ vapor | 1.50 ± 0.02 | 0.001 ± 0.002 | 190 ± 3 | — |
| | 1.0 $M$ KCl | 1.49 ± 0.02 | 0.005 ± 0.005 | 178 ± 3 | 1.0 ± 0.05 |
| C[c] | $N_2$ gas | 1.531 ± 0.005 | 0.007 ± 0.0004 | 251 ± 1 | — |
| | 1.0 $M$ KCl | 1.451 ± 0.006 | 0.005 ± 0.004 | 464 ± 10 | 1.03 ± 0.05 |

[a] $\Gamma = 1.52\ (\pm 0.05) \times 10^{-8}$ mol/cm$^2$, from area of first CV in 1.0 $M$ KCl.
$\Gamma = 1.6\ (\pm 0.2) \times 10^{-8}$ mol/cm$^2$, from area of last deposition CV.
$\tilde{N}_{Pt} = 1.80 - 4.60\hat{\imath}$, $\tilde{N}_{soln} = 1.341 - 0\hat{\imath}$.
[b] $\tilde{N}_{Pt} = 1.85 - 4.25\hat{\imath}$; baked in vacuum oven at 0.01 Torr, 60°C.
[c] $\tilde{N}_{Pt} = 1.86 - 4.15\hat{\imath}$; spin coated from EtOH.

tion[32] but not for a reversible system. (*iv*) The PQ system, like some other redox polymers (plasma-polymerized vinylferrocene,[7,33] PTZ, [30] and TTF [3b,5]), shows unequal forward and reverse conversion rates, possibly as a consequence of changes in film swelling, so it is a good system for testing the importance of changes in swelling on $D_{ct}$.

Film swelling driven by solvent and ion uptake can affect the electrochemical reaction thermodynamics, when the mechanical energy for film expansion (*i.e.*, PV work) is coupled to the energetics of the electrochemical reaction.[34] Changes in $d$ *vs.* oxidation state have been measured by profilometry of dry TTF-functionalized polystyrene films,[5] *in situ* stylus response of a benzylviologen-siloxane polymer,[13] and ellipsometry of polyvinylferrocene[35] and polythionine[16] films; all showed about a 15% increase on conversion to their more charged state. We expect that coupling of the rate of film expansion to the rate of conversion should occur, and such kinetic coupling might contribute to the large differences reported for $D_{ct}$ based on steady-state *vs.* transient methods.[36-38] We monitored $PQ^{2+/+}$ film conversion ellipsometrically as a function of time during potential steps and sweeps to see if slow film swelling was associated with the smaller $D_{ct}$ observed for oxidation.

## Experimental

*Chemicals.*—*N,N'*-bis [-3-(trimethoxysilyl)propyl] 4,4'-bipyridinium dibromide was either prepared in this laboratory by J. G. Gaudiello following published procedures[23] or received as a gift from M. Wrighton. Water was purified with a Milli-Q ion exchange system (Millipore Corporation) equipped with an Organex-Q cartridge and a 0.22 μm final filter. Acetonitrile (MCB Reagents) was vacuum distilled twice from $P_2O_5$ and loaded into the cell in a dry box. All other chemicals were reagent grade and used as received.

*Electrodes.*—The reference electrode was a standard NaCl calomel electrode (SSCE); a large Pt screen served as the counterelectrode. A Pt working electrode (area = 0.164 cm$^2$) was made by brazing a 0.5 mm thick Pt disk (Johnson-Matthey/AESAR, 99.99%) to the end of a brass rod with Ag-based solder before turning down the end in a lathe to 0.180 in. diam. It was then butted against a glass rod of slightly smaller diameter, encased in heat-shrinkable fluorinated ethylene-propylene (FEP) Teflon tubing, and pressed into a tetrafluorethylene (TFE) Teflon cylinder undersized by about 0.025 in. Compression from the undersized TFE Teflon shroud sealed the inner tubing against the Pt/brass rod. The shroud was turned down to 1.000 in. diam and faced-off along with the Pt surface to achieve coplanarity. Successive polishing with 6, 1, and 0.25 μm diamond paste slurries on nylon pads (Buehler, Ltd.) gave a mirror finish. A gold-plated pin connector soldered to the brass rod provided electrical contact. Before each experiment, the electrode was repolished with 1 or 25 μm paste, sonicated in ethanol, cleaned electrochemically by cycling between the potentials for hydrogen and oxygen evolution in degassed 0.5 $M$ $H_2SO_4$, removed at 1.1 V, and rinsed with water.

The ellipsometrically measured complex refractive index ($\tilde{N} = n - k\hat{\imath}$) of the Pt surface varied slightly between experiments because of differences in alignment and the final polishing step. Polishing with 0.25 μm paste, which did not lather well and gave the surface an anomalously high extinction coefficient ($k$ = 4.65) and a slightly angle-dependent refractive index, was used in the surface preparation initially. This was discontinued because a 1.0 μm polish gave more reproducible measurements of $\tilde{N}_{Pt}$ (about 1.86 − 4.20$\hat{\imath}$ in air and in solution, λ = 632.8 nm) which were consistent with reported values for Pt.[39-42]

*Film preparation.*—Film-coated electrodes were prepared either by electroprecipitation of **I** from 0.2 $M$ $K_2HPO_4$/0.1 $M$ KCl solutions (pH 8.9) or by spin coating the surface with a EtOH solution of **I** under a dry $N_2$ blanket. Spin-cast films are noted as such in the table footnotes. Aqueous solutions of **I** were prepared by slowly adding it to water with rapid mixing before adding buffer and adjusting pH, because organotrialkoxysilanes hydrolyze more rapidly in alkaline solution to silane triols, which form cross-linked, colloidal, insoluble polysiloxanols.[43] Electrodeposited films were formed from filtered, *ca.* 3 m$M$ solutions of **I** in $N_2$-purged single compartment cells by repeatedly cycling $E$ between 0.0 and −0.78 V at sweep rates ($v$) of 20 to 100 mV/s. When coated electrodes were studied in a blank 1.0 $M$ KCl solution, they were first rinsed with water and dried briefly in a $N_2$ stream. $\tilde{N}_{Pt}$ is given for each experiment. The uncertainty in $\tilde{N}_{Pt}$ caused by the presence of a native oxide layer changes in interfacial structure as a function of potential, and variations in surface polishing (about 3% of $n$ and $k$) had a negligible effect on estimates of $\tilde{N}$ and $d$ for the film, because the films were thick compared to interfacial layers. Changing $n_{Pt}$ or $k_{Pt}$ by 5% affected estimates of $n$, $k$, and $d$ for films by only 1 to 2%. Following a procedure similar to that used by Willman and Murray to prepare benzylviologen-silane films,[44] we prepared spin-cast films by applying a drop of monomer solution (about 5 mg of **I** per 10 drops of EtOH) while spinning the electrode at 7000 rpm in a photoresist spinner (Model EC101, Headway Research, Inc., Garland, TX). The casting solution was prepared in air, centrifuged for 1 min (Eppendorf Model 5412), and immediately pipetted onto the electrode under $N_2$ gas. New films kept under flowing $N_2$ gas shrank 3% over 12 h. They were cycled twice between dry $N_2$ and air atmospheres to promote hydrolysis, coupling, and cross-linking of the silane groups. Exposure to air caused reversible film swelling of about 140%. Except for film B in Table I, films were not baked, because baking

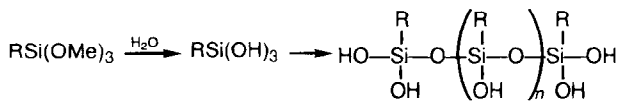


**Scheme I**

did not improve their stability or affect their properties noticeably.

*Optical cell and instrumentation.*—A custom Teflon cell described previously[45] with cylindrical windows for incidence angles ($\Omega$) from 55 to 80° *vs.* surface normal was used for all ellipsometry measurements. The reference electrode was mounted with a Swagelok fitting. An auxiliary solution compartment attached to the top port of the cell housed the counterelectrode and was vigorously purged with $N_2$ without introducing bubbles into the optical path. During vapor swelling measurements, 100% relative humidity was achieved by recirculating the cell atmosphere through a water bubbler with a peristaltic pump.

Ellipsometric measurements were made with a Rudolph Research Model 2437 ellipsometer equipped with a Model RR2000FT rotating analyzer detector, using 632.8 nm light from a 5 mW He-Ne laser. Fast data acquisition rates (27 $\Psi$-$\Delta$ points per second; 37.0 ms/point with an 18.52 ms observation period) and least squares fitting of multiple-thickness data were achieved using software written on a Hewlett-Packard Model 9816S computer. Multiple angle of incidence (MAI) data was fit using the SYSNLIN regression analysis software from the Statistical Analysis Software Institute on an IBM 3081 computer. Electrochemistry was performed using a EG&G Princeton Applied Research Model 175 potential programmer, Model 173 potentiostat, and Model 179 digital coulometer; Hewlett-Packard Model 7045B and Houston Instruments Model 2000 X-Y recorders; and a Norland Model 3001 digital oscilloscope.

## Results

*Monomer electrodeposition.—In situ* ellipsometry was used to monitor film growth during reductive precipitation of **I** from solution. While continuously cycling between reduction and reoxidation of the viologen sites, the ellipsometric angles ($\Psi$ and $\Delta$) were recorded for each $PQ^{2+/+}$ state during film growth (Fig. 1). Data curves A and B were obtained by recording one $\Psi$-$\Delta$ point at each sweep limit of each deposition cycle: $E = -0.75$ and 0.0 V, respectively. Also shown in Fig. 1 are data for the subsequent film swelling (curve C) and dissolution (curve D) that occurred while holding the film in the $PQ^{2+}$ state.

The complex refractive index ($\tilde{N} = n - k\hat{i}$) of the film for each oxidation state was determined by least squares analysis of each data curve, using the overall reflection coefficients for a single, isotropic layer between semi-infinite phases[46] and measured $\tilde{N}$ values for the bare Pt electrode and the solution ($\tilde{N}_{Pt} = 1.81 - 4.65\hat{i}$ and $\tilde{N}_{soln} = 1.337 - 0\hat{i}$).

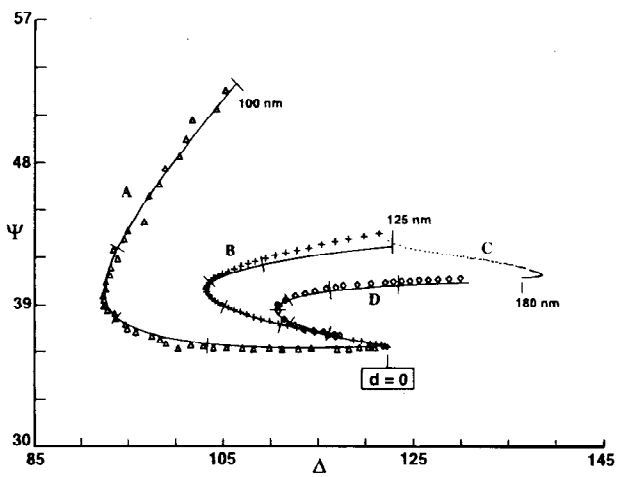


**Fig. 1. Experimental ellipsometric data (points) and calculated (curves) for the (A) 1+ and (B) 2+ states of a $PQ^{2+/+}$ film during growth ($E$ swept continuously from 0.0 to −0.75 V, $v$ = 100 mV/s), (C) subsequent film swelling ($E$ = 0 V) and (D) dissolution. Film $\tilde{N}$ for calculated curves (A) 1.660 − 0.11$\hat{i}$, (B) 1.515 − 0$\hat{i}$, and (D) 1.425 − 0$\hat{i}$. Tick marks indicate 25 nm increments in thickness. $\theta$ = 67°, $\tilde{N}_{Pt}$ = 1.81 − 4.65$\hat{i}$.**

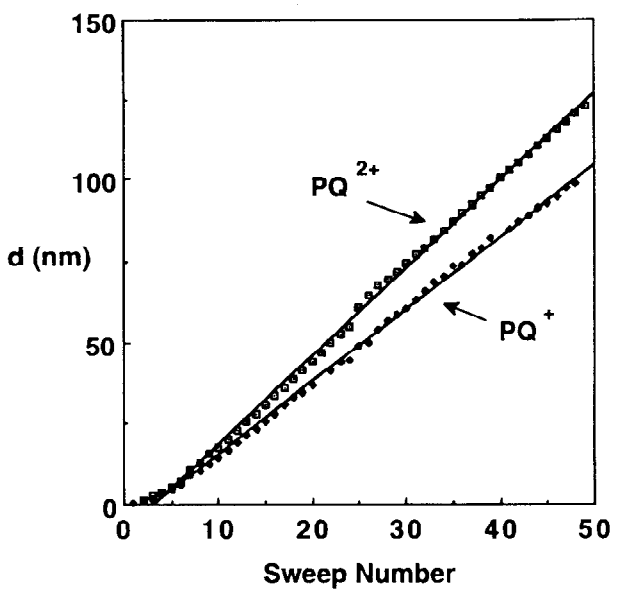


**Fig. 2. Calculated film thicknesses for the data in Fig. 1 *vs.* number of reductive sweeps. Curve fitting gave: $d_{PQ^{2+}} = 2.7 \cdot$ (sweep no.) − 8.4, $d_{PQ^{+}} = 2.2 \cdot$ (sweep no.) − 6.4; $d_{PQ^{+}}/d_{PQ^{2+}} = 77\%$ from ratio of slopes.**

Best fits ($\tilde{N}_{PQ^{+}} = 1.660 - 0.110\hat{i}$ and $\tilde{N}_{PQ^{2+}} = 1.515 - 0\hat{i}$) were obtained by searching a grid of $n$ and $k$ values for the lowest total error sum, where $d$ and the error sum for each $\Psi$-$\Delta$ point ($[\Delta - \Delta_{calc.}]^2 + [\Psi - \Psi_{calc.}]^2$) was found by a line search of $d$ for each set of $n$ and $k$ values. Best fit curves generated by incrementing the film thickness in the reflection equations are shown in Fig. 1 as solid curves over the data points. $k_{PQ^{2+}} = 0$ not only gave the best fits of $PQ^{2+}$ data but also was required for self-consistent fits in which $d$ increased smoothly for points in the bend of the $\Psi$-$\Delta$ plots. The slight deviation of the calculated curve from the data curve for the 2+ state at $d > 75$ nm reflects a small artificial increase in $k_{PQ^{2+}}$ due to incomplete oxidation as the film grew thicker. The agreement of the experimental and theoretical $\Psi$-$\Delta$ data in Fig. 1 and of that (not shown) for thicker films ($d_{PQ^{2+}} > 400$ nm) shows that films deposited isotropically with a constant refractive index for each state. No asymmetric behavior representative of anisotropy of the kind reported for Langmuir-Blodgett films[46b] was observed in $\Psi$-$\Delta$ plots for the transparent (2+) state, even when the plots traversed a complete revolution (*i.e.*, a $2\pi$ change in the film phase thickness).

Scattering by surface roughness was not a problem during potential-sweep depositions, when freshly prepared solutions were used. However, potentiostatic reduction at −0.74 V produced a rough film that scattered the light beam completely when $d$ reached about 70 nm. Varying the sweep rate ($v$ = 20 to 100 mV/s) had no effect on film quality, because there was ample time during each cycle for the $PQ^{2+}$ film to swell and restructure to give a smooth film. Doubling $v$ required about twice as many deposition cycles to reach the same film thickness.

Plots of $d$ *vs.* deposition-cycle number (Fig. 2) were linear after a short induction period, and the ratio of their slopes shows that reduction caused film shrinkage of 33%. Viologen concentrations ($C^*$) for each state were calculated from the charge under voltammetric peaks and corresponding film thicknesses: $C^*_{PQ^{2+}} = 1.4 \pm 0.1$ $M$ and $C^*_{PQ^{+}} = 1.8 \pm 0.1$ $M$. The large error estimates stem from the difficulty of measuring the peak areas for surface-confined groups exclusive of areas for **I** in solution. Peak areas for forward and reverse sweeps were equal, so the change in $C^*$ represents film shrinkage only.

With reference to Fig. 1, ellipsometric data recorded just after the last deposition cycle, while holding $E$ at 0.0 V, show that undried films swelled extensively (curve C) before slowly dissolving back into solution (curve D). The

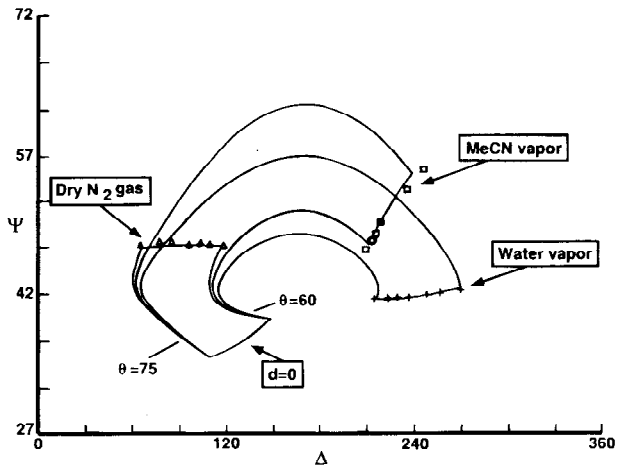


**Fig. 3. MAI data sets (points, θ = 60 to 75°) for $PQ^{2+}$ film as a function of bathing gas and least squares fits: $\tilde{N}$ = 1.667 − 0i, $d$ = 71 nm for dry $N_2$; $\tilde{N}$ = 1.547 − 0i, $d$ = 125 nm for MeCN vapor; and $\tilde{N}$ = 1.410 − 0i, $d$ = 189 nm for water vapor. Also shown are calculated growth curves for θ = 60 and 75° and the MAI curve for bare Pt ($\tilde{N}$ = 1.8 − 4.6i).**

increase in Δ and drop in Ψ in curve C, which began within seconds of stopping $E$ at 0 V and occurred over the 20 min period, represent an increase in $d$ and a drop in $n_{PQ^{2+}}$. Swelling was rapid at first, about half complete in 3 min, and continued for 17 min until dissolution became the dominant process, causing the sharp bend in curve C. A comparison of the least squares fit of multiple angles of incidence (MAI) data recorded in between curves C and D ($n_{PQ^{2+}}$ = 1.440 ± 0.005, $k_{PQ^{2+}}$ = 0.0 ± 0.005, and $d_{PQ^{2+}}$ = 180 ± 5 nm) to the values for the film at the end of the deposition ($n_{PQ^{2+}}$ = 1.515 ± 0.005, $k_{PQ^{2+}}$ = 0.00 ± 0.005, and $d_{PQ^{2+}}$ = 125 ± 5 nm) confirmed that the film became considerably more swollen when not cycled between states. Film dissolution (curve D) was much slower than swelling, only about half complete in 1.5 h, and required 24 h to almost finish (*i.e.*, $d$ = 20 nm). The good fit of the data in curve D by the calculated curve for $n_{PQ^{2+}}$ = 1.425 shows that the film refractive index remained fairly constant during dissolution after dropping initially from 1.44 in 1.5 h. The constancy of $n_{PQ^{2+}}$ suggests that dissolution progressed inward from the film/solution interface, etching the film away without leaching material from within to give increased porosity and associated decrease in $n_{PQ^{2+}}$.

*Solvent swelling and dimerization of $PQ^+$ centers.*—Very stable films and accurate estimates of *in situ* thicknesses and optical constants are required to model transient ellipsometric data meaningfully. Regression analysis of MAI data, which has not been used previously for polymer films, was an excellent way to determine the optical constants and thickness of preformed films. It was particularly convenient for measuring solvent swelling of dried films. Typical MAI data sets for a $PQ^{2+}$ film exposed to different bathing gases, dry $N_2$ gas, acetonitrile vapor, and water vapor, are shown in Fig. 3, along with calculated MAI plots (best fits) drawn at the terminal ends of theoretical film-growth (multiple $d$) plots for the high and low θ of the data set and the corresponding film $\tilde{N}$ values. The film growth curves are shown to illustrate the phase thickness of each film, that is, the location of the data along the periodic Ψ-Δ plots for constant $\tilde{N}$, which is useful in visualizing the dependencies of Ψ and Δ on $n$, $k$, and $d$. Table I summarizes results for a variety of ambient phases. Good estimates of $n$, $k$, and $d$ were obtained except when Δ fell near its inflection point (*i.e.*, its minima) in film growth curves for small $k$ (*i.e.*, $k \leq 0.1$), which occurs at about $d$ = 70 to 90 nm for a range in $n$ typical of polymers ($n$ = 1.7 to 1.4);[47] details are given elsewhere.[45b] In this parameter subspace the dependencies of Ψ on $n$ and $k$ are small and correlated throughout the useful range of θ, making fits somewhat insensitive to $k$ in the range 0 to 0.1. However, the uncertainty in $k$ and consequently in $n$ had only a small effect on the estimate for $d$, so that $d$ = 70 to 90 nm for the dry film data in Fig. 3, the worst case example of MAI data analysis. Dry $PQ^{2+}$ films swelled substantially when exposed to solvent vapors. Vapor from pure water caused film swelling of about 125%, while a 1.0 *M* KCl solution gave only about 90% swelling due to its lower vapor pressure. The thickness of films just after immersion in solution equalled their thickness when swollen by the vapor of that solution.

Although undried films dissolved into the deposition solution, dried films were stable in blank electrolyte solution after substantial initial losses, which probably involved diffusion of monomer and short oligomers out of the film. Break-in cycling in blank electrolyte produced reproducible Ψ-Δ plots and narrower, taller, and more symmetrical cyclic voltammograms (CVs). Fitting MAI data for films completely oxidized and reduced during slow CVs gave precise $\tilde{N}$ and $d$ values for films in blank electrolyte solution. Typical data and best fits are plotted in Fig. 4, along with calculated film growth curves for each oxidation state to show how Ψ and Δ depend on $d$ for each state. Results for two films (A and C in Table I) studied over a few days are summarized in Table II. Reduction caused film shrinkage of 0 to 35%, depending upon the age of the film in solution. Freshly deposited films shrank the most and gave the largest $C^*_{PQ^+}$ values. Break-in cycling caused some film loss and increased $C^*$. Entries in Table II indicate that break-in increased $C^*_{PQ^{2+}}$ by about 20 ± 10%. $PQ^{2+}$ films were significantly more swollen in blank electrolyte solution than during their electrodeposition, as shown by lower $n_{PQ^{2+}}$ and $C^*_{PQ^{2+}}$ values: $n_{PQ^{2+}}$ = 1.46 *vs.* 1.51 and $C^*_{PQ^{2+}}$ = 1.27 *vs.* 1.40 *M*, respectively. $n_{PQ^{2+}}$ for transferred films was almost as low as its value during dissolution of undried films, suggesting that any cross-links formed during film drying did not inhibit swelling.

Treatment of transient Ψ-Δ data requires consideration of the $PQ^+$ monomer-dimer equilibrium, because of its ef-

**Table II. *In situ* film thicknesses, optical constants, and bulk redox concentrations for $PQ^{2+/+}$ films in 1.0 *M* KCl.**

| Film | Redox state | $n$ [a] | $k$ [a] | $d$(nm) [b] | Γ (mol/cm²) [c] | $C^*$ ($M$) [d] | $D_{ct}$ ($10^{-9}$ cm²/s) [e] | Time in soln. |
|---|---|---|---|---|---|---|---|---|
| 1a | $PQ^{2+}$ | 1.457 | 0 | 458 | $4.71 \times 10^{-8}$ | 1.03 | — | 9 h (virgin) |
| 1b | $PQ^{2+}$ | 1.466 | 0 | 301 | $3.79 \times 10^{-8}$ | 1.26 | — | 1 day |
| | $PQ^+$ | 1.717 | 0.178 | 184 | $3.79 \times 10^{-8}$ | 2.06 | — | 1 day |
| 1c | $PQ^{2+}$ | 1.408 | 0.008 | 202 | $2.18 \times 10^{-8}$ | 1.08 | 3.0 | 3 day |
| | $PQ^+$ | 1.519 | 0.145 | 152 | $2.18 \times 10^{-8}$ | 1.43 | 1.0 | 3 day |
| 2a | $PQ^{2+}$ | 1.456 | 0 | 145 | $1.55 \times 10^{-8}$ | 1.07 | — | 5 h (virgin) |
| 2b | $PQ^{2+}$ | 1.457 | 0 | 121 | $1.55 \times 10^{-8}$ | 1.28 | 1.6 | 8 h |
| | $PQ^+$ | 1.508 | 0.115 | 106 | $1.55 \times 10^{-8}$ | 1.46 | 1.2 | 8 h |

Note: Film 1 was spun cast from EtOH solution and film 2 was electrodeposited; $\tilde{N}_{Pt}$ = 1.86 − 4.15i and 1.80 − 4.60i, respectively.
[a] Estimated error of ±0.008.
[b] Estimated error of ~5%.
[c] From peak areas during slow voltammetric sweeps.
[d] Estimated error of ±0.05 *M*.
[e] From chronocoulometry during large amplitude potential steps, using $C^*$ of initial state.

voted in aqueous solutions, at lower temperatures, and at higher viologen radical concentrations[50,55] and can be identified by a blue to violet color shift (absorption $\lambda_{max}$ = 603 nm to $\lambda_{max}$ = 550 nm). Intramolecular dimer formation

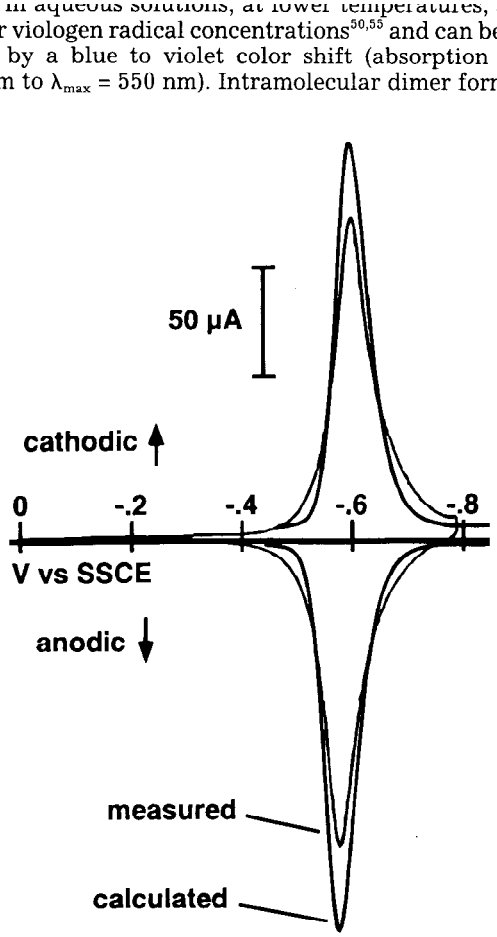


**Fig. 5. Comparison of measured CV peaks for a 140 nm film and theoretical peaks from Eq. 3. $v$ = 50 mV/s, $C^*$ = 1.3 $M$, and K = 7.7 × $10^3$ $M^{-1}$. Calculated peaks are taller and narrower and were drawn separated by 15 mV to align them with measured peaks for easy comparison of peak shapes.**

tion constant for film-bound $PQ^+$ centers (reaction 2). Although theory has been presented for the effects of irreversible dimerization on linear potential-sweep voltammetry of thin-layer systems,[32] we found no treatment of the effects of reversible dimer formation on a nernstian thin-layer system. The expression for this case (see Appendix A) is

$$i/[n^2F^2Vv/4RT] = K^{-1}\theta\{(1 + \theta) - Z\}\{\theta/Z - 1\} \quad [3]$$

where $i$ is the current, $Z = [(1 + \theta)^2 + 8KC^*]^{1/2}$, $\theta = \exp[nF(E - E^{o\prime})/RT]$, $E$ is the electrode potential, $E^{o\prime}$ is the formal potential of the couple in the absence of the dimerization reaction (*i.e.*, in dilute solution), $C^*$ is considered constant (*i.e.*, constant film thickness), $V = A \cdot d$ is the volume of the thin layer, and $K = [(PQ^+)_2]/[PQ^+]^2$ is the dimer formation constant. General analytical expressions for the peak width at half-maximum (FWHM) and peak potential ($E_p$) could not be found, but in the limiting region of $KC^* > 500$

$$E_p = E^{o\prime} + (RT/2nF) \ln (KC^*) \quad [4]$$

$$E_p = E^{o\prime} + (30/n) \log (KC^*) \quad \text{for } T = 25°C \text{ and } E \text{ in mV} \quad [5]$$

Equation 3 predicts symmetrical mirror image oxidation and reduction peaks, positive of $E^{o\prime}$ when the reduced form of the couple undergoes dimerization and negative of $E^{o\prime}$ when the oxidized form undergoes dimerization. Peaks become taller and narrower (limiting FWHM = 66/$n$ mV for $KC^* > 500$) than for a simple nernstian thin layer system (FWHM = 91/$n$ mV).[4]

Experimental CVs for low sweep rates approached the limiting shape predicted by Eq. 3 (see Fig. 5). Calculated CVs for $KC^* = 1 \times 10^4$ closely matched the size, width, and $E_{1/2}$ of experimental CVs, which were 70 mV wide and about 120 mV positive of $E^{o\prime} = -0.69$ V. ($E^{o\prime}$ was estimated from the average peak potentials, $E_{p,c}$ and $E_{p,a}$, for **I** in dilute solutions.) Experimental peaks were slightly shorter and wider than the limiting theoretical shape, because small oxidation-state gradients probably persisted even at this $v$. The measured $C^*$ and shift in $E_{1/2}$ provide a good estimate of $K$: using $C^* = (C^*_{PQ^{2+}} + C^*_{PQ^+})/2 = 1.3$ $M$ gives $K = 7.7$ ($\pm 0.8$) × $10^3$ $M^{-1}$, a value an order of magnitude larger than